Intermetallics 56 (2015) 75–78

Contents lists available at ScienceDirect

Intermetallics

journal homepage: www.elsevier.com/locate/intermet

Magnetic property and magnetocaloric effect in TmCoAl compound

Zhao-Jun Mo [a, b, c], Jun Shen [b, *], Li-Qin Yan [a], Cheng-Chun Tang [c, **], Li-Chen Wang [a], Jian-Feng Wu [b], Ji-Rong Sun [a], Bao-Gen Shen [a]

[a] State Key Laboratory of Magnetism, Beijing National Laboratory for Condensed Matter, Physics and Institute of Physics, Chinese Academy of Sciences, Beijing, China
[b] Key Laboratory of Cryogenics, Technical Institute of Physics and Chemistry, Chinese Academy of Sciences, Beijing, China
[c] School of Material Science and Engineering, Hebei University of Technology, Tianjin, China

ARTICLE INFO

Article history:
Received 7 December 2013
Received in revised form
28 July 2014
Accepted 15 August 2014
Available online 28 September 2014

Keywords:
A. Rare-earth intermetallics
A. Magnetic intermetallics
B. Magnetic properties

ABSTRACT

A large reversible magnetocaloric effect accompanied by a second order magnetic phase transition from paramagnetic (PM) to ferromagnetic (FM) has been observed in TmCoAl intermetallic compound. For the magnetic field change of 5 T, the maximum value of magnetic entropy change ($-\Delta S_M^{max}$) and the value of refrigerant capacity (RC) are evaluated to be 18.2 J/kg K and 211 J/kg, respectively. In particular, a large $-\Delta S_M^{max}$ (10.2 J/kg K) is achieved at 7.5 K under a low magnetic field change from 0 to 2 T with no thermal hysteresis and magnetic hysteresis loss. The large reversible magnetocaloric effect (both the large $-\Delta S_M$ and the high RC) indicates that TmCoAl is one of a promising material for magnetic refrigeration in low temperature.

1. Introduction

The magnetic refrigerator is based on magnetocaloric effect (MCE), which has attracted much attention due to its higher energy-efficiency and lower environmental impact than the conventional gas compression refrigeration [1,2,3]. It is necessary to go on exploring advanced magnetic refrigerant materials with a large magnitude of isothermal magnetic entropy change (ΔS_M) and/or adiabatic temperature change (ΔT_{ad}) for the purpose of magnetic refrigerant application [4]. Up to now, many magnetic materials with large $-\Delta S_M$ have been found, such as $ErCo_2$ [5], $LaFe_{13-x}Si_x$ [6], $MnAs_{1-x}Sb_x$ [7], $MnFeP_{0.45}As_{0.55}$ [8] and $Gd_5Si_2Ge_2$ [9,10] etc. However, most of them are associated with a first-order magnetic or structural phase transition. The first-order phase transition is usually accompanied by a considerable thermal and magnetic hysteresis, which can greatly reduce the actual RC [11,12,13,14]. RC is a crucial parameter for evaluating the technological significance in a refrigerant material. However, materials with a second-order phase transition (SOPT) may have a lower peak value of $-\Delta S_M$, whereas this could be compensated by their large RC due to its thermal and magnetic reversibility. In addition, the permanent magnets in present market can only provide a maximum field of ~2T, and this indicates that a large MCE under low magnetic field change is desirable for the fulfillment of a magnetic refrigerator simply using permanent magnets. Therefore, it is desirable to search new magnetocaloric materials exhibiting a large MCE under low field ($\Delta H \leq 2T$) with a second-order phase transition, such as $ErMn_2Si_2$ [15], $GdNi_4M$ (M = Al, Si) [16], $PrMn_{1.4}Fe_{0.6}Ge_2$ [17] and $TbCo_3B_2$ [18].

The intermetallic ternary compounds of the RTX 1:1:1 type (R = rare-earth, T = transition metal, X = p-metal) have been devoted much effort to study. The RTX exhibit a very rich variety of crystallographic structures. Among the RTX compounds, the RCoAl were found to crystallize in the more densely packed hexagonal Laves phase $MgZn_2$-type structure [19]. RCoAl compounds have been reported to show anisotropic lattice expansion/contraction as a function of temperature which could affect their magnetic and transport properties [20]. Magnetic and magnetocaloric properties of RCoAl (R = Gd, Tb, Dy and Ho) have been studied. Under a magnetic field change of 5 T from zero field, the values of $-\Delta S_M^{max}$ are 10.4, 12.5, 16.3, and 21.5 J/Kg K for the RCoAl (R = Gd, Tb, Dy, and Ho) alloys, respectively [21]. In the present paper, we report a study on the magnetic and magnetocaloric properties of TmCoAl alloy. The large reversible $-\Delta S_M^{max}$ (10.2 J/Kg K) with zero thermal hysteresis and magnetic hysteresis is achieved for a low magnetic field change of 2 T. The RC value of the TmCoAl is increased with the increasing field changes and reached to 72 and 211 J/kg for the field

* Corresponding author.
** Corresponding author.
E-mail address: jshen@mail.ipc.ac.cn (J. Shen).

http://dx.doi.org/10.1016/j.intermet.2014.08.006
0966-9795/

changes of 2 and 5 T, respectively. The results imply TmCoAl compound is expected to have effective applications in low temperature magnetic refrigeration.

2. Experiments

The polycrystalline sample of TmCoAl compound was synthesized by arc melting of stoichiometric amounts of the elements Tm, Co and Al (99.9%) under a purified argon atmosphere on a water-cooled copper hearth using a titanium zirconium alloy as a getter (The content of Tm was 3% more than the theoretical value). The ingot was melted three times with the button being turned over after each melting to ensure the homogeneity. The sample was annealed at 1123 K for 10 days, and a subsequent quenching to room temperature was performed to obtain crystalline samples. Powder X-ray diffraction (XRD) measurements were performed at room temperature by using Cu Kα radiation to identify the crystal structure and the lattice parameters. Magnetizations were measured by employing a commercial superconducting quantum interference device (SQUID) magnetometer, model MPMS-7 from Quantum Design Inc.

3. Results and discussion

Fig. 1 shows the Rietveld refined powder XRD patterns of TmCoAl compound at room temperature. The refinement shows that the prepared sample is of single phase. The compound TmCoAl crystallizes in the hexagonal $MgZn_2$-type crystal structure (space group $P6_3/mmc$, No. 194). In this structure, the Tm has an unique crystallographic site (4f); the Co and Al atoms statistically occupy the sites of 2a and 6h, respectively. The lattice parameters are determined to be $a = 5.2714$ (2) Å and $c = 8.4593$ (7) Å with $R_{wp} = 4.5\%$ by the Rietveld technique using GSAS program.

Fig. 2 shows the typical temperature dependences of the magnetization M (T) curves for TmCoAl compounds under an applied magnetic field of $H = 0.01$ T. The TmCoAl compound exhibits a magnetic transition from ferromagnetic (FM) to paramagnetic (PM), and the Curie temperature (T_C) is determined to be 6 K, defined as the maximum slope of M-T curve. It can be seen that there is almost no thermal hysteresis between the ZFC and FC curves as observed usually in SOPT, when the temperature increases above T_C. However, a significant thermal irreversibility is

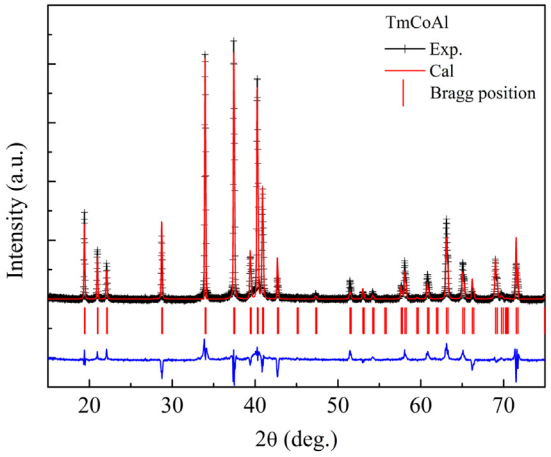

Fig. 1. Rietveld refined powder XRD patterns of TmCoAl compound at room temperature. The observed data is indicated by cross line, and the calculated profile is the straight line overlying them. The short vertical bar indicates the Bragg peak position of TmCoAl. The lower curve shows the difference between the observed and calculated intensities.

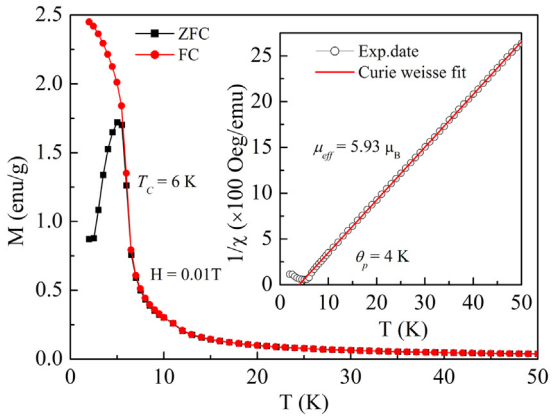

Fig. 2. Temperature dependences of ZFC and FC magnetizations of TmCoAl under the magnetic field of 0.01 T. Inset: the temperature variation of the ZFC inverse susceptibility fitted to the Curie–Weiss law.

clearly observed below T_C. The thermomagnetic irreversibility can be observed in many cases, such as, spin-glass systems, materials with competing magnetic interactions, and materials with high anisotropy and low ordering temperature [22], where the domain wall width could be comparable to that of lattice spacing, thus resulting in a large pinning effect [21]. Considering the magnetic anisotropy due to the large orbital angular momentum in Tm atoms (or ions) and low T_C for TmCoAl, the thermomagnetic irreversibility is likely arising from the narrow domain wall pinning effect. The inset of Fig. 1 shows the reciprocal magnetic susceptibility χ_m^{-1} versus temperature for TmCoAl. The magnetic susceptibility of the TmCoAl compound at temperatures above 10 K follows the Curie–Weiss law $\chi_m^{-1} = (T - \theta_p)/C_m$. Here θ_p is the PM Curie temperature and C_m is the Curie–Weiss constant. The value of θ_p for TmCoAl is 4 K, which is lower than T_C in spite of the ferromagnetic ordering at low temperature. It indicates that the indirect RKKY-type exchange interaction is mainly responsible for magnetic order in these materials [23]. Previous studies have shown that the magnetic contribution of the Co atoms could be neglected because of the filling of the d band by aluminum electrons in the hexagonal $MgZn_2$ structure, which is a close-packed Laves phase [24]. The effective magnetic moment μ_{eff} per Tm atom (5.93 μ_B) is obtained based on the value of C_m. This value is smaller than the free-ion value for Tm^{3+} (7.1 μ_B) due to the crystal field effects and magnetic anisotropy.

Fig. 3(a) shows the isothermal magnetization curves as a function of magnetic field, which were measured in applied fields of up to 5 T in a temperature range from 2 to 26 K. It can be seen from Fig. 3(a) that there is a considerable difference in the M–H curves for TmCoAl compound in different temperature ranges. In the 18–26 K temperature ranges, the field dependence of the magnetization shows a linear relation, whereas the isothermal curves for $T_C < T < 18$ K shows an appreciable nonlinearity. The curvatures in the M–H curves above T_C probably indicate the existence of short-range FM correlations in the PM state, which is in agreement with the result of positive θ_p for TmCoAl compound (see Fig. 2). It should be noticed that although the isothermal magnetization curves are gradually saturated with increasing magnetic fields at considerably lower fields below T_C, the complete saturation is not observed at 5 T. The lack of complete saturation in TmCoAl compound is likely attributed to the strong anisotropy and the crystalline electric field. The magnetic moment value per Tm atom at 2 K and 5 T reaches about 4.0 μ_B, which is close to that reported in Ref. [25] and this is much smaller than the theoretical ordered state magnetic moment (7.1 μ_B) of Tm^{3+} ion. This reduction in ordered state moment might

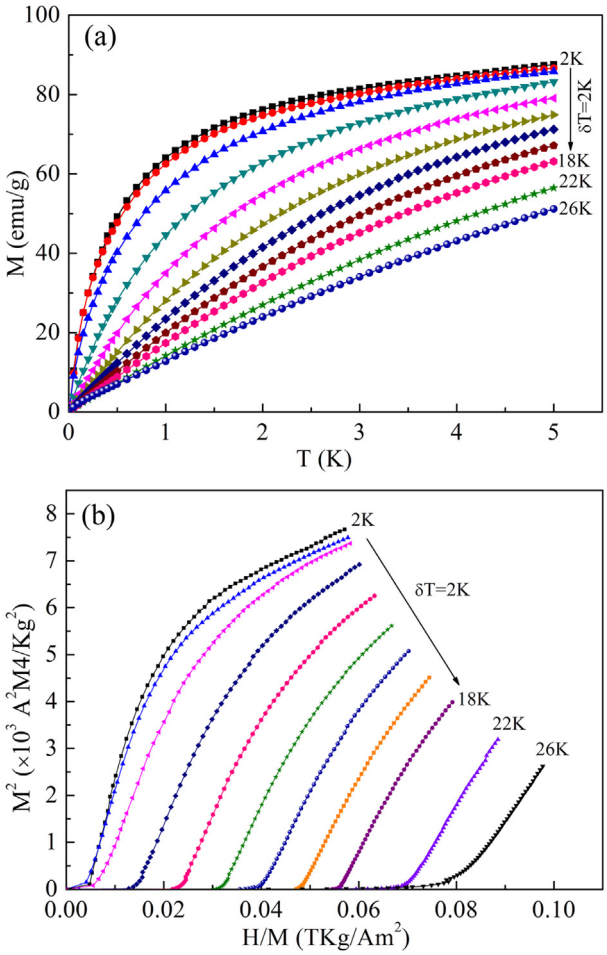

Fig. 3. Magnetization isotherms and the Arrott plots of TmCoAl collected in the temperature range of 2–26 K.

stem from the crystal field effects and magnetic anisotropy. Another possibility is the giant intrinsic hardness proposed earlier for TmCoAl compound related to the crystallographic randomization which results from the high magnetic anisotropy and exchange fluctuation [26]. In TmCoAl compound there is a considerable local disorder because of the statistical distribution of Co and Al at 6h sites. Hence, the 4*f*-4*f* indirect exchange interaction that is mediated by the conduction electrons may have some intrinsic

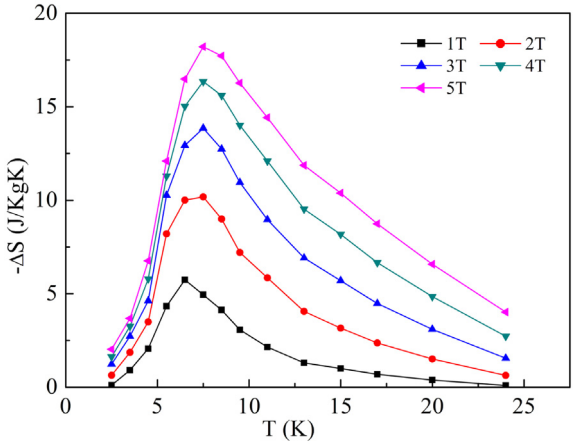

Fig. 4. Temperature dependences of magnetic entropy changes in TmCoAl for different magnetic field changes.

Table 1
The magnetic order transition temperature (T), $-\Delta S_M{}^{max}$ and RC with the field change of 2 T for TmCoAl and other MCE materials around 10 K.

Compounds	T (K)	Order of transition	$-\Delta S_M$ (J/kg K)	RC (J/kg)	Refs.
$ErRu_2Si_2$	5.5	First	11	55	[29]
$HoNi_2B_2C$	6.5	First	5.7	62	[30]
$DyCo_2B_2$	10	Second	4.5	0.9 (J/cm^3)	[31]
DyCuSi	10	First	~10.5	~160	[32]
$Eu_8Ga_{16}Ge_{30}$	10	Second	8.0	80	[11]
HoCoAl	10	–	12.5	–	[21]
$Dy_{0.9}Tm_{0.1}Ni_2B_2C$	9.2	First	4.05	52	[33]
TmCoAl	7.5	Second	10.2	~72	Present

randomness associated with the statistical occupancy of 6h site. Fig. 3(b) shows the Arrott plot of the TmCoAl compound in the temperature range of 2–26 K. As is well known, according to the Banwejee criterion [27], a magnetic transition is expected to be of the first order when the slope of M^2 versus H/M plot is negative, whereas it will be of the second order when the slope is positive. Neither negative slope nor inflection point is observed in the Arrott plots of TmCoAl, indicating a characteristic of second-order FM-PM magnetic transition.

The MCE in terms of isothermal magnetic entropy change has been determined by utilizing Maxwell's relationship $\Delta S(T,H) = \int_0^H (\partial M/\partial T)_H dH$ in which T is the absolute temperature and H is the applied field. The values of $-\Delta S_M$ for different magnetic field changes as a function of temperature are showed in Fig. 4. The value of $-\Delta S_M^{max}$ is found to increase monotonically with the increase of applied magnetic field. For the magnetic field change of 5 T, the value of $-\Delta S_M^{max}$ is 18.2 J/kg K at 7.5 K, which is just above the boiling point of helium. Particularly, the value of $-\Delta S_M^{max}$ is found to be 10.2 J/kg K under a low magnetic change of 2 T, this value is larger than 4.9 J/kg K for GdCoAl, 5.3 J/kg K for TbCoAl and 9.2 J/kg K for DyCoAl. Although the values of $-\Delta S_M^{max}$ are 12.5 J/kg K and 21.5 J/kg K around 20 K for HoCoAl under the field change 2 and 5T, respectively. The temperature is near the boiling point of hydrogen (20.4 K). The TmCoAl compound has confirmed a characteristic of second-order FM-PM magnetic transition, no thermal hysteresis and zero field hysteresis. The low field MCE parameters of TmCoAl are comparable or larger than those of most potential magnetic refrigerant materials in a similar magnetic transition temperature which are listed in Table 1. Moreover, the $-\Delta S_M$ does not die out even at temperatures well above T_C, possibly due to the presence of spin fluctuations [28]. The RC is considered to be another important requirement of a potential magnetic refrigerant, which is a measure of how much heat can be transferred between the cold and hot sinks in one ideal refrigerant cycle [34]. The value of RC is defined as $RC = \int_{T_1}^{T_2} |\Delta S_M| dT$, where T_1 and T_2 are the temperatures corresponding to both sides of the half-maximum value of $-\Delta S_M$ peak, respectively. One can find that the RC value of the TmCoAl increases with the increasing field changes and reaches to 72 and 211 J/kg, for the field changes of 0–2 and 0–5T, respectively. This RC value is higher than that (55 J/kg) of $ErRu_2Si_2$, which is 55 J/kg calculated for a field change of 0–2T in Ref. [29]. Our results suggest the TmCoAl compound could be a very attractive candidate material by using in a magnetic refrigerator working at low temperature.

4. Conclusion

In summary, the polycrystalline TmCoAl intermetallic compound with a single phase has been synthesized. The magnetic

property and MCE are investigated. A large reversible MCE without thermal and magnetic hysteresis loss has been observed in TmCoAl compound, which originates from the second order magnetic phase transition from PM to FM. With the magnetic field change of 0–5 T, the values of $-\Delta S_M^{max}$ is evaluated to be 18.2 J/kg K and the maximum value of RC is 211 J/kg. In particular, a large $-\Delta S_M^{max}$ and RC values are 10.2 J/kg K and 72 J/kg at 7.5 K under a magnetic field change from 0 to 2 T, respectively, which is important for the practical application of the TmCoAl compound in low-temperatures. The present results indicate that TmCoAl is one of a promising candidate for magnetic refrigeration in low temperature, particularly for helium liquefaction.

Acknowledgments

This work was supported by the National Basic Research Program of China (No. 2011AA03A404), the National Natural Science Foundation of China (No. 51322605; No. 11104337; No. 51271192; No. 11274357), and the Knowledge Innovation Project of the Chinese Academy of Sciences.

References

[1] Brück E. J Phys D Appl Phys 2005;38:R381.
[2] Pecharsky VK, Gschneidner Jr KA. J Magn Magn Mater 1999;200:44.
[3] Gschneidner Jr KA, Pecharsky VK, Tsoko AO. Rep Prog Phys 2005;68:1479.
[4] Gutfleisch O, Willard MA, Brück E, Chen CH, Sankar SG, Ping Liu J. Adv Mater 2011;23:821.
[5] Hu FX, Shen BG, Sun JR, Chen ZH, Rao GH, Zhang XX. Appl Phys Lett 2001;78:3675.
[6] Tegus O, Brück E, Buschow KHJ, de Boer FR. Nature 2002;415:150.
[7] Wada H, Tanabe Y. Appl Phys Lett 2001;79:3302.
[8] Pecharsky VK, Holm AP, Gschneidner Jr KA, Rink R. Phys Rev Lett 2003;91:198.
[9] Pecharsky VK, Gschneidner Jr KA. Phys Rev Lett 1997;78:4494.
[10] Pecharsky VK, Gschneidenr Jr KA. Appl Phys Lett 1997;70:3299.
[11] Phan MH, Woods GT, Chaturvedi A, Stefanoski S, Nolas GS, Srikanth H. Appl Phys Lett 2008;93:252505.
[12] Tegus O, Bruck E, Buschow KHJ, De Boer FR. Nature (London) 2002;415:150.
[13] Gama S, de Campos A, Coelho AA, Alves CS, Ren Y, Gacia F, et al. Adv Funct Mater 2009;19:942.
[14] Zou JD, Shen BG, Gao B, Shen J, Sun JR. Adv Mater 2009;21:693.
[15] Li L, Nishimura K, Hutchison WD, Qian Z, Huo D, Namiki T. Appl Phys Lett 2012;100:152403.
[16] Toliński T, Falkowski M, Synoradzki K, Hoser A, Stüßer N. J Alloys Compd 2012;523:43–8.
[17] Zeng R, Dou SX, Wang JL, Campbell SJ. J Alloys Compd 2011;509:119–23.
[18] Li L, Huo D, Igawa H, Nishimura K. J Alloys Compd 2011;509:1796–9.
[19] Oesterreicher H. J Less-Common Met 1971;25:228.
[20] Jarosz J, Talik E, Mydlarz T, Kusz J, Bohm H, Winiarski A. J Magn Magn Mater 2000;208:169.
[21] Zhang XX, Wang FW, Wen GH. J Phys Condens Matter 2001;13:L747.
[22] Zhang H, Shen BG, Xu ZY, Shen J, Hu FX, Sun JR, et al. Appl Phys Lett 2013;102:092401.
[23] Prchal Jiří, Javorský P, Dopita M, Isnard O, Sechovský V. J Alloys Comp 2006;408:155–7.
[24] Chiu LB, Elliston PR, Stewart AM, Taylor KNR, Issa MAA. J Phys F 1980;10:2297.
[25] Oesterreicher H. J Less-Common Met 1977;55:199–204.
[26] Oesterreicher H, Pitts R. J Appl Phys 1972;43:5174.
[27] Banerjee SK. Phys Lett 1964;12:16.
[28] Kumar P, Singh NK, Nayak AK, Haldar A, Suresh KG, Nigam AK. J Appl Phys 2010;107:09A932.
[29] Samanta T, Das I, Banerjee S. Appl Phys Lett 2007;91:152506.
[30] Li L, Nishimura K, Huo D, Kadonaga M, Namiki T, Qian Z. Appl Phys Exp 2011;4:093101.
[31] Li L, Nishimura K, Usui G, Huo D, Qian ZH. Intermetallics 2012;23:101–5.
[32] Chen J, Shen BG, Dong QY, Sun JR. Solid State Commun 2010;150:1429–31.
[33] Li L, Nishimura K. Appl Phys Lett 2009;95:132505.
[34] Shen BG, Sun JR, Hu FX, Zhang HW, Chen ZH. Adv Mater 2009;21:4545.